Electrochemical Modification of Vertically Aligned Carbon Nanotube Arrays

X. R. Ye,[†] L. H. Chen,[†] C. Wang,[‡] J. F. Aubuchon,[†] I. C. Chen,[†] A. I. Gapin,[†] J. B. Talbot,*[,†] and S. Jin*[,†]

Materials Science & Engineering, University of California, San Diego, 9500 Gilman Drive, La Jolla, California 92093-0411, and Pacific Northwest National Laboratory, Environmental Molecular Sciences Laboratory, P.O. Box 999, K8-93, Richland, Washington 99352

Received: December 25, 2005; In Final Form: May 5, 2006

Electrochemical oxidation and reduction were utilized to modify vertically aligned carbon nanotube (CNT) arrays grown on a porous network of conductive carbon microfibers. Ultrafast and complete CNT opening and purification were achieved through electrochemical oxidation. Highly dispersed platinum nanoparticles were then uniformly and densely deposited as electrocatalysts onto the surface of these CNTs through electrochemical reduction. Using supercritical drying techniques, we demonstrate that the unidirectionally aligned and laterally spaced geometry of the CNT arrays can be fully retained after being subjected to each step of electrochemical modification. The open-tipped CNTs can also be electrochemically detached in full lengths from the supporting substrates and harvested if needed.

Introduction

Aligned carbon nanotube (CNT) arrays offer distinct advantages to a broad range of potential applications in comparison with loose and randomly oriented CNT powders that often need assembly or integration.[1,2] Well-aligned, densely arrayed but mutually separated CNTs grown directly on a conductive and porous substrate are ideal for constructing high-surface-area electrodes for polymer electrolyte membrane fuel cells (PEMFCs).[3−5] As electrical conduction paths between all the CNTs and the current collector have already been established, the preparation procedure of electrodes is simplified, and the local blockage of gas or liquid supply to the electrodes is minimized. Electrocatalysts supported by such CNT arrays not only achieve a high dispersion but also have simultaneous access to the gas, the electron-conducting medium, and the proton-conducting medium, resulting in a significant enhancement of the performance and utilization efficiency of the electrocatalysts. The importance of aligned CNTs grown on conductive substrates for the development of amperometric chemical sensors and biosensors has also been explored.[1,6,7] The conductive substrate provides a direct transduction platform for signal monitoring, and the CNTs serve as matrixes for molecule immobilization. Promoted electron transfer is thus established between the active site of immobilized molecules and the underlying electrochemical transducer through the aligned CNT mediators, leading to excellent overall sensing characteristics. Moreover, vertically aligned CNT arrays possess more efficient electron emission and offer an additional advantage of device integration for field emitters.[1] Obviously, maintaining the desired vertical orientation would facilitate the implementation of CNT arrays as fuel cell electrodes, sensor platforms, field emitter components, and other applications.

Well-aligned CNT arrays are produced mainly by dc plasma-enhanced chemical vapor deposition (PECVD).[8,9] Normally, the tips of the as-grown CNTs are capped by the metal seed catalysts (such as Ni, Co, or Fe) and also often with amorphous carbon coatings which may degrade CNT properties. The surfaces of the as-grown CNTs are pristine. CNT modifications, such as tip opening, purification, functionalization, and decoration, are therefore essential to enable particular CNT array-based applications. Tip opening and purification get rid of the metal impurities and amorphous carbon inherent to the as-grown CNTs, thus eliminating the anticipated deleterious or poisonous effect of metal impurities on the long-term reliability of electrochemical reactions at CNT-based fuel cell electrodes. For biosensor applications, the removal of biotoxic metals will improve the biocompatability of CNTs and avoid the potential interference of metal impurities with sensing procedures. The sharp edge of CNTs generated by tip opening and purification exhibits enhanced field emission due to field concentration[10,11] and can be utilized for selective functionlization or decoration of CNT ends.[6,7] The hollow interior of CNTs can also be made available by tip opening and purification to incorporate foreign materials.[12] In fuel cell and sensor applications, efficient catalyst loading and/or molecule immobilization can be achieved through functionalization or decoration of CNTs at the open ends, into the inner channels, and on the external surface.[5,12,13]

Various approaches have been well-established for the modification of CNTs.[14−19] The harsh and solvent-intensive treatment in the most typically used wet chemical modification, as well as the natural drying process, when applied to the well-aligned but free-standing CNT arrays, usually causes undesirable agglomeration/bundling of CNTs or even total collapse of aligned and laterally separated geometry.[4,20] Dry modification techniques can retain the alignment of CNT arrays; however, most of them are less efficient, flexible, or convenient than the wet chemical process.[19]

We have succeeded in fabrication of vertically aligned three-dimensional CNT arrays on a porous network of conductive carbon microfibers.[21] Our CNTs were grown by dc plasma-enhanced CVD, and hence have a herringbone structure. To make these aligned CNT arrays more suitable for fuel cell

* To whom correspondence should be addressed. E-mail: jtalbot@ucsd.edu (J.T.); jin@ucsd.edu (S.J.).
[†] University of California, San Diego.
[‡] Pacific Northwest National Laboratory.

10.1021/jp057507m CCC: $33.50
Published on Web 06/14/2006

electrodes and other potential applications, we devised a simple electrochemical method to modify the CNT arrays with minimal damage or disruption to CNTs themselves and the aligned geometry. Quick removal of metal seed catalysts and amorphous carbon from the CNT ends and consequently CNT opening were achieved through electrochemical oxidation. Highly dispersed, ultrafine nanoparticles of platinum were uniformly and densely deposited onto the sidewalls of the open-tipped and purified CNTs through electrochemical reduction. Supercritical CO_2 ($scCO_2$) drying techniques retained the vertically aligned and laterally spaced geometry of these free-standing CNT arrays after the wet processing. Also, the open-tipped and purified CNTs can be electrochemically removed from the supporting substrates and harvested.

Experimental Section

Vertically aligned CNT (with herringbone structure) arrays were grown on a carbon microfiber network by nickel-catalyzed decomposition of acetylene through dc plasma-enhanced CVD, according to a procedure described elsewhere.[8,9,21] The electrically conductive carbon microfiber, a woven mat consisting of $\sim$5 μm diameter fibers (hitherto referred to as carbon paper), was procured from ElectroChem. Inc. Electrochemical oxidation for tip opening and purification of CNT arrays was performed in an aqueous solution of 57% H_2SO_4 at room temperature. The cathode was a 0.5 cm^2 platinum sheet, and the anode was a 0.5 cm^2 carbon paper substrate with the arrayed CNTs grown unidirectionally perpendicular to the substrate along the applied electric field direction. The electrodes were placed vertically, parallel to each other, and connected to a dc power supply. Following the electrochemical oxidation, Pt was deposited onto the CNT samples through electrochemical reduction using a three-electrode dc method in 5 mM H_2PtCl_6 and 0.5 M H_2SO_4 aqueous solution.[22] The deposition potential used was 0 V vs SCE (standard calomel electrode) and the loading of Pt was controlled by the total charge applied.

After electrochemical modification, the CNT samples were washed several times with distilled water and ethanol. During all these steps, the samples were kept in the solution. The CNT samples were quickly transferred to a 10 mL autoclave filled with ethanol. The ethanol in the CNT samples was then replaced with liquid CO_2. After the autoclave was filled with liquid CO_2 and the residual ethanol was at or below the 10 ppm level, the temperature of the autoclave was increased to 45 °C in 2 h with the pressure reaching about 100 bar. The samples were maintained at 100 bar and 45 °C for 3 h. Finally, CO_2 was transformed from supercritical to the gas phase by decreasing the pressure to atmospheric pressure at the same temperature. For comparison, natural drying in a vacuum or air was also performed.

The surface morphologies of the as-grown vs electrochemically modified CNT arrays were examined using a Phillips field emission scanning electron microscope (SEM) with an accelerating voltage of 10−30 kV. Transmission electron microscopy (TEM) analysis of the CNTs was carried out with a JEOL JEM 2010 microscope with a routine point-to-point resolution of 0.194 nm. The operating voltage of the microscope was 200 keV. All images were digitally recorded with a slow scan CCD camera (image size 1024 × 1024 pixels) and image processing was carried out using a Digital Micrograph (Gatan). The TEM samples were prepared by scraping CNTs from the substrate and then dispersing in ethanol, followed by dropping a small amount of the slurry on a holey carbon-coated copper grid and drying.

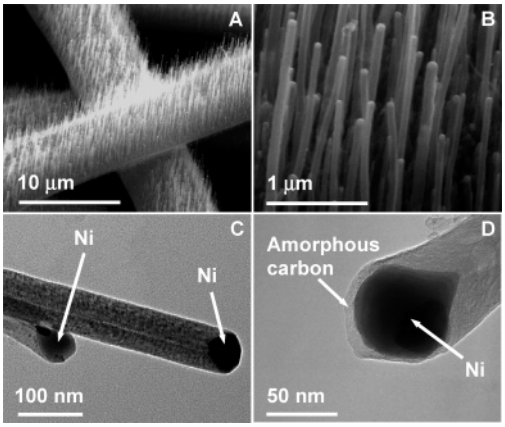

Figure 1. (A) Low- and (B) high-magnification SEM images of as-grown CNT arrays on a carbon paper substrate. (C) and (D) TEM images of Ni nanoparticles and amorphous carbon caps on as-grown CNT tips.

Results and Discussion

Figures 1A and 1B show the typical morphology of the as-grown CNT arrays with a vertically aligned and laterally separated structure on a carbon paper substrate. The CNT arrays are three-dimensional since, in the carbon paper substrate, the woven and pasted carbon microfibers cross over each other and form a three-dimensional porous network. Most CNTs are quite straight and up to several micrometers in length. The outer diameters of CNTs ranged from 30 to 100 nm. A tip-growth mechanism was responsible for the formation of the CNTs with the catalyst Ni nanoparticles located on the top of the nanotubes. A TEM micrograph of Figure 1C indicates that the typical as-grown CNTs, with an inner diameter of about 6−10 nm, were closed by elongated conical or pear-shaped catalyst Ni nanoparticles. A thin amorphous carbon layer capped the catalyst nanoparticles for some CNT tips, as shown in Figure 1D.

Figures 2A−2C are SEM images of the CNT arrays on carbon paper substrates after electrochemical oxidation and ethanol rinsing followed by natural drying in air or in a vacuum. The electrochemical treatment proceeded for 20 s using a 57% H_2SO_4 solution and 1 mA current. As can be seen from Figures 2A and 2B, the CNTs were bent, clustered, and severely agglomerated after the electrochemical process and subsequent drying, although the nanotubes are completely opened and no metal catalyst nanoparticles or amorphous carbon are left on the tips, as shown in Figure 2C. The reason for the observed change in CNT morphology is that the CNTs are exposed to air or vacuum after the environmental liquids are evaporated, and the surface tension force exerted on each high-aspect-ratio CNT leads to the agglomeration of the CNTs and the collapse of aligned geometry into entangled heavy stacks. A general trend was noted that the disordering extent of the CNT arrays increased with the evaporation rate of the environmental liquid. Such agglomeration and collapse are highly undesirable as a major portion of the CNT surface is now blocked and less accessible for electrochemical reactions. The collapsed CNT arrays are also expected to have less electric field enhancement than vertically aligned CNT arrays with individual and separated CNTs.[23]

To avoid CNT agglomeration and collapse caused by the liquid−gas interface, a $scCO_2$ drying step was introduced after the electrochemical oxidation of CNTs to eliminate the surface tension force during the evaporation of the ethanol. As is evident from Figures 3A and 3B, the CNT tips are now open while maintaining the essential structure of the aligned and mutually

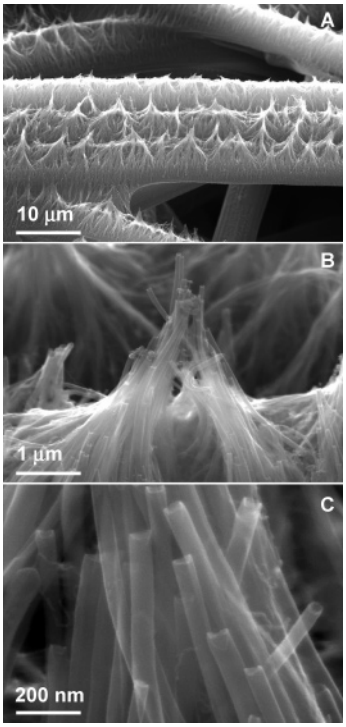

Figure 2. SEM images of (A and B) severely agglomerated and (C) completely opened CNT arrays on carbon paper substrates after electrochemical oxidation and ethanol rinsing followed by drying in air or in a vacuum.

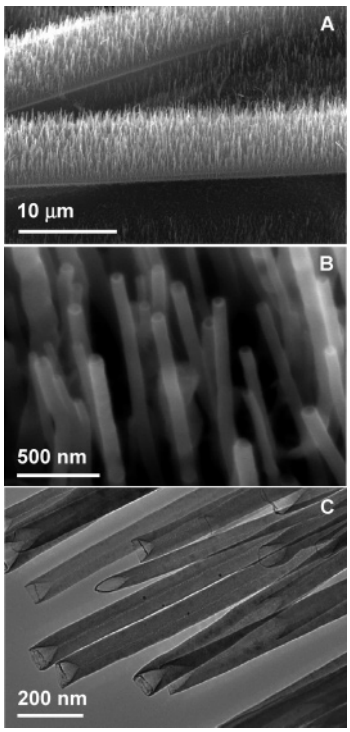

Figure 3. (A) and (B) SEM micrographs of aligned and separated nanotubes after tip opening and supercritical CO_2 drying. (C) TEM images of open-tipped CNTs.

separated CNT configuration. The severely bundled nanotubes previously seen in Figure 2A and 2B are no longer present in the $scCO_2$ dried samples. Furthermore, such results imply that the electrochemical oxidation itself is not the cause of CNT agglomeration, but the natural drying process is. Figure 3C is a TEM image of the CNTs after electrochemical oxidation. Ni seed nanoparticles, as well as the amorphous carbon layer caps,

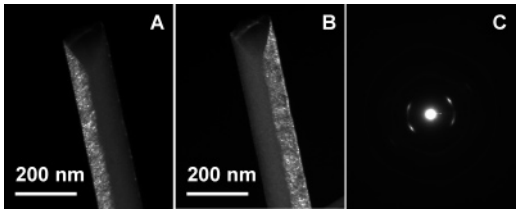

Figure 4. (A) and (B) Dark field TEM images and (C) electron diffraction of representative open-tipped CNTs.

were removed and all the tips were opened; no obvious structural changes of CNTs were observed. It is also noticeable from Figure 3C that the tip opening caused the sharp edges of the CNT tips to be exposed, which could enhance electron field emission due to the increased field concentration effect. The average radius of curvature in the open tipped nanotubes, e.g., of the order of several nanometers such as that seen in Figure 3C, is obviously significantly smaller than the broad radius of curvature defined by the catalyst particle at the tip of the unopened nanotubes, e.g., of ~30 nm.

The herringbone structure of a representative open-tipped CNT is revealed by the dark field TEM imaging and electron diffraction shown in Figure 4. The dark field images were taken by tilting the beam to pass part of the graphite 002 ring through the objective aperture. Only one side of the CNT is bright in each of the two dark field images, indicating that the graphite lattice planes are correctly oriented to diffract into the objective aperture on only one side of the CNT. The electron diffraction was typified by two sets of intensity arc and dark field imaging reveals that each of these arcs in the diffraction pattern was related to half section of the fiber. All these verify that the CNT have a herringbone structure, with the graphite lattice planes inclined to the CNT axis.

The relative purity of the CNTs in terms of the Ni catalyst contents has been compared before vs after electrochemical oxidation using inductively coupled plasma-mass spectrometry (ICP-MS). Metal impurities from CNTs were dissolved in HNO_3 solutions with identical volume and concentration. Based on ICP-MS analysis, the Ni concentrations in HNO_3 solution were 115 720 and 1389 ppb (ng/g) per 1 $in.^2$ area of the as-grown and the electrochemically oxidized CNT samples, respectively. The results indicate that 98.8% of Ni has been removed by electrochemical oxidation. Since the aligned CNTs served as anodes in electrochemical oxidation, and their orientation was parallel to the electric field direction, the reactions occurring preferentially on CNT tips enabled the efficient etching of amorphous carbon and Ni seed catalyst. The positively charged Ni cations, as soon as they were produced, were expelled away from CNTs and dissolved into aqueous solution of H_2SO_4. Even as described by previous research of others that there might be some oxygen-containing functional groups produced on the surface of CNTs upon electrochemical oxidation,[24] Ni ions and H_2SO_4 solution, possibly adsorbed on a CNT surface, can be removed by subsequent washing with water, a simple method that has been proven effective in a similar situation, cleaning CNTs after chemical oxidation/purification in HNO_3 or a mixture of HNO_3 and H_2SO_4.

We have compared the effect of electrochemical vs chemical oxidation for CNT tip opening and purification. In 57% H_2SO_4 aqueous solution at room temperature, the removal of the catalyst particles and resultant nanotube tip opening are basically completed within an extremely short time of just ~2 s when a constant current of 2 mA was applied. With chemical etching alone without applying current, as arrows in Figure 5A indicate,

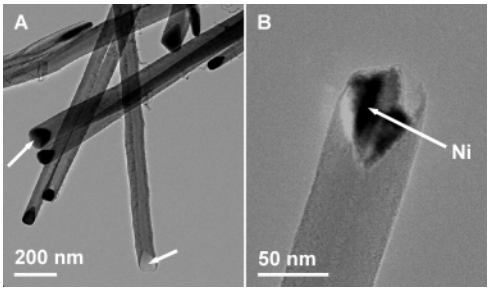

Figure 5. TEM images of CNTs after (A) 5 min and (B) 1 h of chemical etching in 57% H_2SO_4 solution.

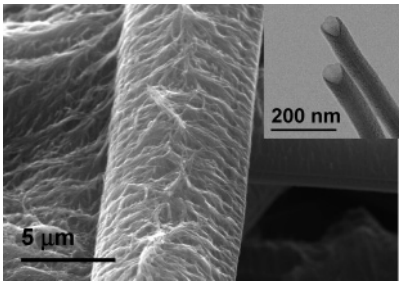

Figure 6. SEM image of agglomerated CNTs after 1 h of chemical etching in hot HNO_3 solution and subsequent $scCO_2$ drying. The inset is a TEM image showing opened CNT tips.

partial or complete removal of Ni nanoparticles was beginning to be seen only on a small number of CNTs after 5 min, and the catalyst particles on many CNT tips were not completely removed even after ~1 h of etching time (Figure 5B). Obviously, electrochemical oxidation offers significant advantages as it is at least 2−3 orders of magnitude faster than chemical etching for CNT tip opening and purification in 57% H_2SO_4. For the chemical etching using 57% H_2SO_4 at room temperature, the amorphous carbon is chemically inert to the neutral acid H_2SO_4, and the oxidation of the exposed Ni seed catalyst depends mostly on the dissolved oxygen, resulting in a poor tip opening and CNT purification process. Likewise, chemical etching in reducing acids such as HCl is inefficient for tip opening and metal removal. As in the case of chemical etching using oxidizing acids such as HNO_3 or a mixture of HNO_3 with H_2SO_4, a relatively long period of time is still necessary to ensure the complete CNT opening and purification due to the slow attack of the oxidizing acids on amorphous carbon and Ni at room temperature. Chemical etching in hot HNO_3 or a mixture of HNO_3 with H_2SO_4 is more efficient for CNT opening and purification. As indicated by the inset of Figure 6, no metal catalyst nanoparticles or amorphous carbon is left on the tips, and the nanotubes are completely opened after 1 h of chemical etching in hot HNO_3. However, the original alignment of CNT arrays totally collapsed; even the sample was $scCO_2$ dried (Figure 6). The CNTs entangled with each other to form a highly compact mess. Compared to such a traditional liquid-phase chemical oxidation process using concentrated HNO_3 or a mixture with H_2SO_4 at refluxing temperature, the electrochemical method demonstrated is mild and more environmentally benign. Due to the highly efficient and rapid electrochemical etching of amorphous carbon and the seed catalyst, the long hours of severe chemical treatment and nanotube agglomeration are avoided.

Since the tip opening and purification of CNT arrays is caused by electrochemical oxidation, we have preliminarily evaluated other types of electrochemical baths besides the 57% H_2SO_4 solution used here. A series of electrolyte solutions, such as 5% H_2SO_4, 5% HNO_3, 25% HNO_3 + 25% H_2SO_4, 5% H_3PO_4, 5% CH_3COOH, 5% EDTA, 5% $KMnO_4$, and 5% KOH, have been tested for electrochemical opening of CNT tips at room temperature. The efficiency is highly dependent on the electrolytes being utilized. When the electrochemical oxidation was performed in neutral or basic aqueous solutions, such as 5% EDTA, 5% $KMnO_4$, and 5% KOH, no significant tip opening was observed. As has been confirmed in the literature,[25,26] although the amorphous carbon can be eliminated effectively upon the electrochemical oxidation occurring preferentially at the end regions of CNTs, the exposed growth catalyst Ni was most likely converted to nickel oxides,[26] which are poorly soluble in neutral or basic aqueous solutions. A subsequent washing in acidic solutions such as HCl or H_2SO_4 is necessary to dissolve the oxidized growth catalyst.[26] If aqueous solutions of common strong or modest acids, 5% H_2SO_4, 5% HNO_3, or 25% HNO_3 + 25% H_2SO_4, 5% H_3PO_4 and 5% CH_3COOH were used for electrochemical oxidation; not only the amorphous carbon can be readily etched[27] but also the oxidized growth catalyst can be dissolved. Therefore, Ni can be removed feasibly from the CNT tips to achieve complete tip opening and significant purification of CNTs. This is consistent with the phenomena reported by other researchers.[28] The results were reproducible despite the wide difference in the nature of the acids and concentrations, but the optimal etching conditions varied. Nevertheless, the TEM images of the etched CNTs were similar to those in Figure 3C. There was also no major collapse of CNT alignment after supercritical drying.

To study the effect of electrochemical oxidation at higher current density, the CNT arrays on a carbon paper substrate were also subjected to electrochemical oxidation in 57% H_2SO_4 solution using a 200 mA for 20 s. It has been found that the CNTs were not only opened and purified but also lifted off from the substrate and suspended in the electrochemical bath. This lift-off phenomenon can be utilized as a convenient means to harvest open-tipped and purified CNTs with essentially similar lengths by simply increasing the current density. SEM (image not shown) examination of the harvested CNTs demonstrated that, compared to the original CNTs, the whole CNT length was essentially intact after electrochemical harvesting.

Since the electrochemical tip opening and purification does not cause significant CNT agglomeration and collapse of alignment on the substrate, further electrochemical modification of CNTs was performed directly thereafter to achieve functionalization and decoration of CNT arrays. Figure 7A shows the SEM image of the CNT arrays after the Pt electrodeposition with 0.1 mg/cm^2 Pt loading and subsequent $scCO_2$ drying. Again, the aligned geometry of CNT arrays is essentially retained after the Pt deposition. It is seen from Figure 7A that highly dispersed Pt nanoparticles are uniformly deposited on the sidewalls of each CNT. From the bright-field TEM images displayed in Figure 7B and 7C, the average diameter of these particles appears to be around 10 nm. The lattice fringe image in Figure 7C further confirms the herringbone structure expected of the CNT support. It is apparent that the CNT consists of graphite platelets that are aligned in an angle with respect to the CNT axis. Many edges of the stacking graphenes can be observed in the surface of the CNTs. The spacing between the graphitic platelets was 0.34 nm, which correspond to that of graphite, 0.335 nm.[29] Furthermore, the structural integrity of CNTs is maintained throughout the electroplating.

The successful tip opening and purification, and the successful Pt deposition, indicate good electrical contacts between Pt electrocatalyst and CNTs, as well as those between CNTs and the substrate. Therefore, such open-tipped and purified CNT

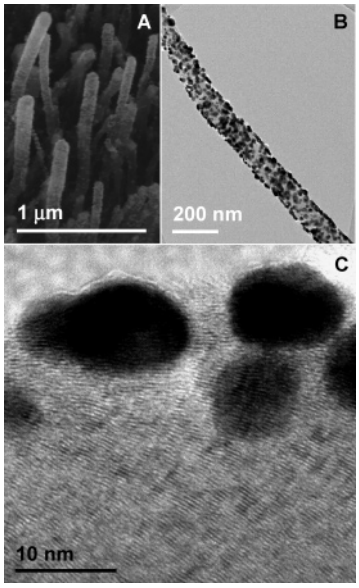

Figure 7. Electron micrographs of aligned and separated CNTs after tip opening, Pt electrodeposition, and supercritical CO_2 drying: (A) SEM, (B) low-magnification TEM, and (C) high-magnification TEM.

arrays with vertically aligned and mutually separated geometry on a conductive and porous network of carbon microfibers, provide an ideal platform for constructing the active layer of membrane electrodes for PEMFCs. Our electrochemical modification approach described here also ensures that the open-tipped and purified CNT arrays are in direct contact with the conductive substrate underneath and other species or materials attached/immobilized on CNTs, and produces continuous pathways for carrier transport. Therefore, these CNT arrays can be useful for fabricating other electrically driven nanodevices, such as biosensors, bioactuators, battery electrodes, and so forth.

Conclusion

In summary, an electrochemical approach has been developed to produce modified, nonagglomerated, and three-dimensional free-standing CNT arrays vertically aligned on a porous network of conductive carbon microfibers. Ultrafast and highly efficient CNT opening and purification were achieved through electrochemical oxidation. Highly dispersed Pt nanoparticles were then uniformly and densely deposited onto the sidewalls of such CNT arrays through electrochemical reduction. The unidirectionally aligned and laterally spaced geometry of CNT arrays was fully retained in each step of electrochemical modification, and the supercritical drying process prevented undesirable bundling/agglomeration of CNTs after the electrochemical process. A high-current electrochemical process to completely lift off the CNTs from the substrate was also demonstrated for harvesting open-tipped and purified CNTs with the whole CNT length essentially intact.

Acknowledgment. The support of this work by NSF-NIRTs under Grant Nos. DMI-0210559 and DMI-0303790, UC Discovery Fund under Grant No. ELE02-10133/Jin, Iwama Endowed Fund at UC San Diego, Lawrence Livermore National Laboratory under Grant No. MI-04-006, and DuPont is acknowledged. The TEM work was carried out at EMSL of Pacific Northwest National Laboratory.

References and Notes

(1) Melechko, A. V.; Merkulov, V. I.; McKnight, T. E.; Guillorn, M. A.; Klein, K. L.; Lowndes, D. H.; Simpson, M. L. *J. Appl. Phys.* **2005**, *97*, 041301/1.

(2) Dai, L.; Patil, A.; Gong, X.; Guo, Z.; Liu, L.; Liu, Y.; Zhu, D. *ChemPhysChem.* **2003**, *4*, 1151.

(3) Wang, C.; Waje, M.; Wang, X.; Tang, J. M.; Haddon, R. C.; Yan, Y. S. Nano Lett. 2004, 4, 345; Wang, X.; Waje, M.; Yan, Y. S. *Electrochem., Solid-State Lett.* **2005**, *8*, A42.

(4) Tang, H.; Chen, J. H.; Huang, Z. P.; Wang, D. Z.; Ren, Z. F.; Nie, L. H.; Kuang, Y. F.; Yao, S. Z. *Carbon* **2004**, *42*, 191. Tang, H.; Chen, J. H.; Yao, S. Z.; Nie, L. H.; Kuang, Y. F.; Huang, Z. P.; Wang, D. Z.; Ren, Z. F. *Mater. Chem., Phys.* **2005**, *92*, 548.

(5) Ye, X. R.; Lin, Y.; Wai, C. M.; Talbot, J. B.; Jin, S. *J. Nanosci. Nanotechnol.* **2005**, *5*, 964.

(6) Sotiropoulou, S.; Chaniotakis, N. A. *Anal. Bioanal. Chem.* **2003**, *375*, 103.

(7) Li, J.; Koehne, J. E.; Cassell, A. M.; Chen, H.; Ng, H. T.; Ye, Q.; Fan, W.; Han, J.; Meyyappan, M. *Electroanalysis* **2005**, *17*, 15.

(8) AuBuchon, J. F.; Chen, L. H.; Gapin, A. I.; Kim, D. W.; Daraio, C.; Jin, S. *Nano Lett.* **2004**, *4*, 1781.

(9) Chen, L. H.; AuBuchon, J. F.; Gapin, A. I.; Daraio, C.; Bandaru, P.; Jin, S.; Kim, D. W.; Yoo, I. K. *Appl. Phys. Lett.* **2004**, *85*, 5373.

(10) Rinzler, A. G.; Hafner, J. H.; Nikolaev, P.; Lou, L.; Kim, S. G.; Tomanek, D.; Nordlander, P.; Colbert, D. T.; Smalley, R. E. *Science* **1995**, *269*, 1550.

(11) Wang, Q. H.; Corrigan, T. D.; Dai, J. Y.; Chang, R. P. H.; Krauss, A. R. *Appl. Phys. Lett.* **1997**, *70*, 3308.

(12) Ye, X. R.; Lin, Y.; Wang, C.; Wai, C. M. *Adv. Mater.* **2003**, *15*, 316.

(13) Ye, X. R.; Wai, C. M.; Lin, Y. *Chem. Commun.* **2003**, 642. Ye, X. R.; Lin, Y.; Wang, C.; Engelhard, M. H.; Wai, C. M. *J. Mater. Chem.* **2004**, *14*, 908. Lin, Y.; Cui, X.; Ye, X. R. *Electrochem. Commun.* **2005**, *7*, 267.

(14) Dillon, A. C.; Gennett, T.; Jones, K. M.; Alleman, J. L.; Parilla, P. A.; Heben, M. J. *Adv. Mater.* **1999**, *11*, 1354.

(15) Ebbesen, T. W.; Ajayan, P. M.; Hiura, H.; Tanigaki, K. *Nature* **1994**, *367*, 519.

(16) Hinds, B. J.; Chopra, N.; Rantell, T.; Andrews, R.; Gavalas, V.; Bachas, L. G. *Science* **2004**, *303*, 62.

(17) Dumitrica, T.; Garcia, M. E.; Jeschke, H. O.; Yakobson, B. I. *Phys. Rev. Lett.* **2004**, *92*, 117401.

(18) Chen, Q.; Dai, L.; Gao, M.; Huang, S.; Mau, A. W. H. *J. Phys. Chem. B* **2001**, *105*, 618.

(19) Sun, C. L.; Chen, L. C.; Su, M. C.; Hong, L. S.; Chyan, O.; Hsu, C. Y.; Chen, K. H.; Chang, T. F.; Chang, L. *Chem. Mater.* **2005**, *17*, 3749.

(20) Li, Z. J.; Pan, Z. W.; Dai, S. *J. Colloid Interface Sci.* **2004**, *277*, 35. Soundarrajan, P.; Patil, A.; Dai, L. M. *J. Vac. Sci. Technol.* **2003**, *21*, 1198. Nguyen, C. V.; Delzeit, L.; Cassell, A. M.; Li, J.; Han, J.; Meyyappan, M. *Nano Lett.* **2002**, *2*, 1079.

(21) Chen, L. H.; Aubuchon, J. F.; Ye, X. R.; Chen, I. C.; Gapin, A. I.; Jin, S. *Appl. Phys. Lett.* **2006**, *88*, 033103/1−033103/3.

(22) Thompson, S. D.; Jordan, L. R.; Shukla, A. K.; Forsyth, M. *J. Electroanal. Chem.* **2001**, *515*, 61.

(23) Tzeng, Y.; Chen, Y.; Sathitsuksanoh, N.; Liu, C. *Diamond Relat. Mater.* **2004**, *13*, 1281.

(24) Ye, J. S.; Liu, X.; Cui, H. F.; Zhang, W. D.; Sheu, F. S.; Lim, T. M. *Electrochem. Commun.* **2005**, *7*, 249. Liu, P.; Hu, J. *Sensors Actuators B* **2002**, *84*, 194. Barisci, J. N.; Wallace, G. G.; Baughman, R. H. *J. Electroanal. Chem.* **2000**, *488*, 92. Hinds, B. J.; Chopra, N.; Rantell, T.; Andrews, R.; Gavalas, V.; Bachas, L. G. *Science* **2004**, *303*, 62. Lefrant, S.; Baibarac, M.; Baltog, I.; Mevellec, J. Y.; Mihut, L.; Chauvet, O. *Synth. Met.* **2004**, *144*, 133. Unger, E.; Graham, A.; Kreupl, F.; Liebau, M.; Hoenlein, W. *Curr. Appl. Phys.* **2002**, *2*, 107. Li, C.; Wang, D.; Wang, X.; Liang, J. *Carbon* **2005**, *43*, 1557.

(25) Ito, T.; Sun, L.; Crooks, R. M. *Electrochem. Solid-State Lett.* **2003**, *6*, C4.

(26) Fang, H. T.; Liu, C. G.; Liu, C.; Li, F.; Liu, M.; Cheng, H. M. *Chem. Mater.* **2004**, *16*, 5744.

(27) Yang, Z. H.; Wu, H. Q.; Li, J.; Li, X. H. *Chem. J. Chin. Univ.* **2001**, *22*, 446.

(28) Skowronski, J. M.; Scharff, P.; Pfander, N.; Cui, S. *Adv. Mater.* **2003**, *15*, 55.

(29) Rodriguez, N. M.; Chambers, A.; Baker, R. T. K. *Langmuir* **1995**, *11*, 3862.